THE JOURNAL OF BIOLOGICAL CHEMISTRY VOL. 281, NO. 3, pp. 1808–1816, January 20, 2006

Conversion of Green Fluorescent Protein into a Toxic, Aggregation-prone Protein by C-terminal Addition of a Short Peptide*[S]

Received for publication, May 23, 2005, and in revised form, October 18, 2005 Published, JBC Papers in Press, October 19, 2005, DOI 10.1074/jbc.M505581200

Christopher D. Link[‡1], Virginia Fonte[‡], Brian Hiester[‡], John Yerg[‡], Jmil Ferguson[‡], Susan Csontos[§], Michael A. Silverman[§], and Gretchen H. Stein[¶]

From the [‡]Institute for Behavioral Genetics, University of Colorado, Boulder, Colorado 80309, [§]Biological Sciences, California State Polytechnic University, Pomona, California 91768, and [¶]Molecular, Cellular, and Developmental Biology, University of Colorado, Boulder, Colorado 80309

A non-natural 16-residue "degron" peptide has been reported to convey proteasome-dependent degradation when fused to proteins expressed in yeast (Gilon, T., Chomsky, O., and Kulka, R. (2000) *Mol. Cell. Biol.* 20, 7214–7219) or when fused to green fluorescent protein (GFP) and expressed in mammalian cells (Bence, N. F., Sampat, R. M., and Kopito, R. R. (2001) *Science* 292, 1552–1555). We find that expression of the GFP::degron in *Caenorhabditis elegans* muscle or neurons results in the formation of stable perinuclear deposits. Similar perinuclear deposition of GFP::degron was also observed upon transfection of primary rat hippocampal neurons or mouse Neuro2A cells. The generality of this observation was supported by transfection of HEK 293 cells with both GFP::degron and DsRed(monomer)::degron constructs. GFP::degron expressed in *C. elegans* is less soluble than unmodified GFP and induces the small chaperone protein HSP-16, which co-localizes and co-immunoprecipitates with GFP::degron deposits. Induction of GFP::degron in *C. elegans* muscle leads to rapid paralysis, demonstrating the *in vivo* toxicity of this aggregating variant. This paralysis is suppressed by co-expression of HSP-16, which dramatically alters the subcellular distribution of GFP::degron. Our results suggest that in *C. elegans*, and perhaps in mammalian cells, the degron peptide is not a specific proteasome-targeting signal but acts instead by altering GFP secondary or tertiary structure, resulting in an aggregation-prone form recognized by the chaperone system. This altered form of GFP can form toxic aggregates if its expression level exceeds the capacity of chaperone-based degradation pathways. GFP::degron may serve as an instructive "generic" aggregating control protein for studies of disease-associated aggregating proteins, such as huntingtin, α-synuclein, and the β-amyloid peptide.

Aggregating proteins or peptides have been associated with numerous neurodegenerative diseases (1), although the molecular mechanisms remain unclear. The apparent toxicity of these protein aggregates has been demonstrated in cell culture and in many transgenic mouse and invertebrate models (reviewed in Refs. 2–4). We have shown previously that transgenic expression of the human β-amyloid peptide (Aβ)[2] in *Caenorhabditis elegans* leads to the formation of intracellular aggregates and associated toxicity (5). Similar observations have been made for transgenic *C. elegans* animals expressing polyglutamine repeat proteins (6–8), α-synuclein (9), or tau (10). One unanswered question for the *C. elegans* (as well as *Drosophila* and mammalian) disease models is the specificity of the observed toxicity, *i.e.* would *any* aggregating protein have the same effect? In theory, this question could be addressed by control experiments in which transgenic animals are constructed in parallel that express a nondisease-associated, "generic" aggregating protein. We show here that GFP can be converted into such a control aggregating protein and that expression of this aggregating GFP variant results in *in vivo* toxicity grossly similar to that observed for disease-associated aggregating proteins.

In a search for random peptides that would confer instability on proteins expressed in yeast, Gilon *et al.* (11) identified a non-natural 16-residue peptide (CL1) that conferred apparent ubiquitin-dependent degradation on the Ura3 protein. This short C-terminal "degron" peptide was subsequently used by Bence *et al.* (12) to engineer an unstable GFP variant (GFP-u) that underwent proteasome-dependent degradation in HEK 293 cells. When we attempted to engineer a similar construct to monitor proteasome function in *C. elegans*, we unexpectedly found that GFP::degron fusion protein aggressively formed persistent, perinuclear aggregates. We have therefore taken advantage of this unexpected result, and we used this novel, aggregating derivative of GFP to examine the generic response to protein aggregation in a *C. elegans* model.

EXPERIMENTAL PROCEDURES

DNA Constructions—The initial GFP::degron fusion was generated using *C. elegans* expression vector pPD118.20 (gift of A. Fire), which expresses a Ser-65 → Cys GFP variant under the control of the *C. elegans myo-3* promoter. A synthetic double-stranded oligonucleotide encoding the 16-residue CL1 degron peptide (cGCATGCAAGAACTGGTTCTCTAGCCTGTCCCACTTCGTCATCCATCTGTAGg), bracketed by EcoRI- and NheI-compatible single-stranded extensions, was ligated to EcoRI/NheI-cleaved pPD118.20, resulting in the *myo-3*/GFP::degron vector pAT2. Blunt-end ligation was used to generate a control plasmid (pAT1) that contained a 7-nucleotide insert upstream of

* This work was supported by National Institutes of Health Grants AG12423 and AG21037 (to C. D. L.), Alzheimer Disease Research Grant A2003-209 from the American Health Assistance Foundation (to G. H. S.), and NIH Grant R15 NS048047a and a California State University faculty-student research grant (to M. A. S.). The costs of publication of this article were defrayed in part by the payment of page charges. This article must therefore be hereby marked "*advertisement*" in accordance with 18 U.S.C. Section 1734 solely to indicate this fact.

[S] The on-line version of this article (available at http://www.jbc.org) contains Fig. S1.

[1] To whom correspondence should be addressed: Institute for Behavioral Genetics, University of Colorado, UCB 447, Boulder, CO 80309. Tel.: 303-735-5112; Fax: 303-492-8063; E-mail: linkc@colorado.edu.

[2] The abbreviations used are: Aβ, β-amyloid peptide; GFP, green fluorescent protein; EGFP, enhanced GFP; DAPI, 4,6-diamidino-2-phenylindole; GFP-u, unstable GFP; Bis-Tris, 2-[bis(2-hydroxyethyl)amino]-2-(hydroxymethyl)propane-1,3-diol; MES, 4-morpholineethanesulfonic acid; CMV, cytomegalovirus; DIC, differential interference microscopy.

the degron sequence, resulting in an out-of-frame degron peptide. To generate a myo-3/GFP::PEST expression construct, the mouse ornithine decarboxylase 1 PEST region was recovered by PCR and inserted into the EcoRI/NheI sites of pPD118.20 as described above. To generate a GFP::degron construct with pan-neuronal expression, the *myo-3* promoter region of pAT2 was replaced with a PstI/XbaI fragment from pCL35 (containing the *snb-1* promoter and a synthetic 3′-untranslated intron), resulting in construct pCL54. Temperature-inducible expression of the GFP::degron was engineered by replacing a KpnI/NheI fragment of *smg*-1-dependent *myo-3* vector pPD118.60 (encoding unmodified GFP) with a KpnI/NheI fragment of pAT2 containing the GFP::degron fusion, resulting in pCL60.

To express the GFP::degron fusion protein in mammalian cells, an EcoRI/BstEI restriction fragment encoding the degron peptide was recovered from pCL54 and inserted into the downstream EcoRI/XmaI sites of vector pEGFP-C2 (Clontech). The resulting construct, pCL85, expresses an EGFP::degron protein under control of the CMV promoter. To engineer mammalian DsRed::degron expression, an AgeI/EcoRI fragment from the pDsRed monomer (Clontech) encoding the DsRed monomer protein was swapped for the EGFP in pCL85. The DsRed stop codon was then removed by *in vitro* mutagenesis (QuickChange kit, Stratagene), fusing the degron peptide in-frame with the DsRed monomer protein. The terminal peptide sequences of all expression constructs used in this study are shown in Table 1. For clarity, we will refer to the CMV-driven EGFP constructs as "GFP" in the text of this work, with the understanding that these constructs express the sequence-modified EGFP.

To engineer constitutive expression of HSP-16 in *C. elegans* muscle, the coding region of the *hsp-16.2* gene (including its single intron) was amplified from genomic DNA and inserted between the KpnI and EcoRI sites of pPD118.20, thus replacing GFP with the *hsp-16.2* coding sequence, generating pCL137. All constructions were checked by DNA sequencing.

Construction of Transgenic C. elegans Strains—Transgenic lines were generated by microinjection of the constructs described above. Plasmid pRF4, encoding dominant *rol-6*(*su250*) mutant collagen, was co-injected as a selectable morphological marker for all microinjections, with one exception; pCL137 (*myo-3*/*hsp-16.2*) was co-injected with a GFP marker plasmid (pCL26 (*mtl-2*/GFP)) that produces strong intestinal GFP expression. Lines with chromosomally integrated transgenes were generated by γ-irradiation as described previously (5).

DNA Transfection of Mouse N2A Cells and Primary Rat Hippocampal Neurons—Neuro2a (N2A) cells were seeded on polylysine-coated coverslips at 1.25×10^5 cells/cm^2 in minimum Eagle's medium-α + 10% fetal bovine serum (without antibiotics) and transfected a day later with either pEGFP-C2 vector (Clontech) or pCL85 (pEGFP-C2::degron (pAT2)) using Lipofectamine 2000 (Invitrogen).

Primary cultures of dissociated neurons from E18 embryonic rat hippocampi were prepared essentially as described (13). Cells were maintained in Neurobasal medium (Invitrogen) supplemented with B-27 and Glutamax. After 7 days *in vitro*, cells were transfected with 2.0 μg of plasmid DNA using Lipofectamine 2000, as per the manufacturer's instruction. Cells were maintained in a 37 °C, 5% CO_2 incubator for 12 or 24 h to allow for protein expression.

Transfection of HEK 293 Cells and Analysis of GFP and DsRed Aggregates—Human embryonic kidney cells (HEK 293-H, Invitrogen) were seeded on collagen-coated Dulbecco's modified Eagle's medium coverslips at 2.5×10^5 cells/cm^2 in Dulbecco's modified Eagle's medium + non-essential amino acids + 10% fetal bovine serum (without antibiotics). One day later, they were transfected with Lipofectamine 2000 and a total of 2–4 μg of plasmid DNA using various combinations of the following plasmids: pEGFP-C2, pCL85 (EGFP::degron), pDsRed(monomer), pCL169 (DsRed(monomer)::degron), and pGFP-u (a gift from R. Kopito (12)). Expression of each construct was examined singly and in combination with a control for the transfection efficiency, *i.e.* the GFP-degron DNAs (pCL85 and pGFP-u) and plain GFP (pEGFP-C2) were co-transfected with plain DsRed(monomer) as a control for transfection efficiency, and conversely, DsRed(monomer)::degron (pCL169) was cotransfected with plain GFP (pEGFP-C2). After 17 h, the cells were fixed with 10% paraformaldehyde for 20–30 min at room temperature, permeabilized, and stained with DAPI.

The coverslips were examined by epifluorescence, and images of the EGFP, DsRed(monomer) and DAPI fluorescence were obtained as described below. These images were scored experiment-blind for the number of cells containing aggregated EGFP and the number containing aggregated DsRed. These values were normalized to the relative number of transfected cells by using the masking function of SlideBook software to determine the area in μm^2 occupied by the fluor serving as the control for transfection efficiency.

As a further check on the results obtained by scoring the images blind, we devised a simple algorithm to detect aggregates objectively. We determined the mean intensity of both GFP and DsRed(monomer) in the area masked by the control fluor, we then set the threshold for visualization of each fluor at four times its mean intensity. The small points of fluorescence that exceeded that "4× threshold" generally corresponded to aggregates identified by eye, but the following two issues made it less accurate than the human eye. First, cells with intense fluorescence exceeded the 4× threshold regardless of whether they contained any aggregates (false positives). Some of these false positives were eliminated by specifying that true aggregates do not lie over the nuclei nor extend over more than half the cell. Second, some cells with weak overall fluorescence contained clear aggregates that did not exceed the 4× threshold, which was based on the mean intensity of the population as a whole (false negatives). Despite the limitations of the algorithm-based approach, these objective measurements of aggregates paralleled the experiment-blind human scoring, validating our scoring methods.

Immunofluorescence and Light Microscopy—Nematode populations were fixed in 4% paraformaldehyde and permeabilized using a 2-mercaptoethanol/collagenase treatment as described previously (5). Permeabilized worms were probed with polyclonal rabbit HSP-16 antibody (14) at 1:500 dilution and Texas Red-conjugated secondary antibody (1:100, Molecular Probes). Nematode (and live N2A cell) images were acquired with a Zeiss Axioskop epifluorescence microscope equipped with 40× air (NA 0.75) and 100× (NA1.3) oil Plan Neofluor objectives and a digital deconvolution retrofit (Intelligent Imaging Innovations).

For comparison of GFP fluorescence distribution in transfected primary neurons, three cultures were analyzed for both GFP and GFP::degron transfections. Exposure times were adjusted so that cell body fluorescence was within the linear range of the camera, and that cell body fluorescence was comparable between GFP and GFP::degron-transfected neurons. Fluorescence in all control GFP-transfected neurons was readily detectable in the distal axons and dendrites (12 of 12 cells, fluorescence at least 4× higher than background), whereas fluorescence in GFP::degron-transfected cells was not detectable in these neurites above background (14 cells analyzed).

Hippocampal cells were fixed in a solution of 4% paraformaldehyde, 4% sucrose in phosphate-buffered saline and then blocked in 0.5% fish skin gelatin in phosphate-buffered saline for 1 h at 37 °C. After blocking, coverslips were incubated with a polyclonal MAP2 (1:500, Chemicon

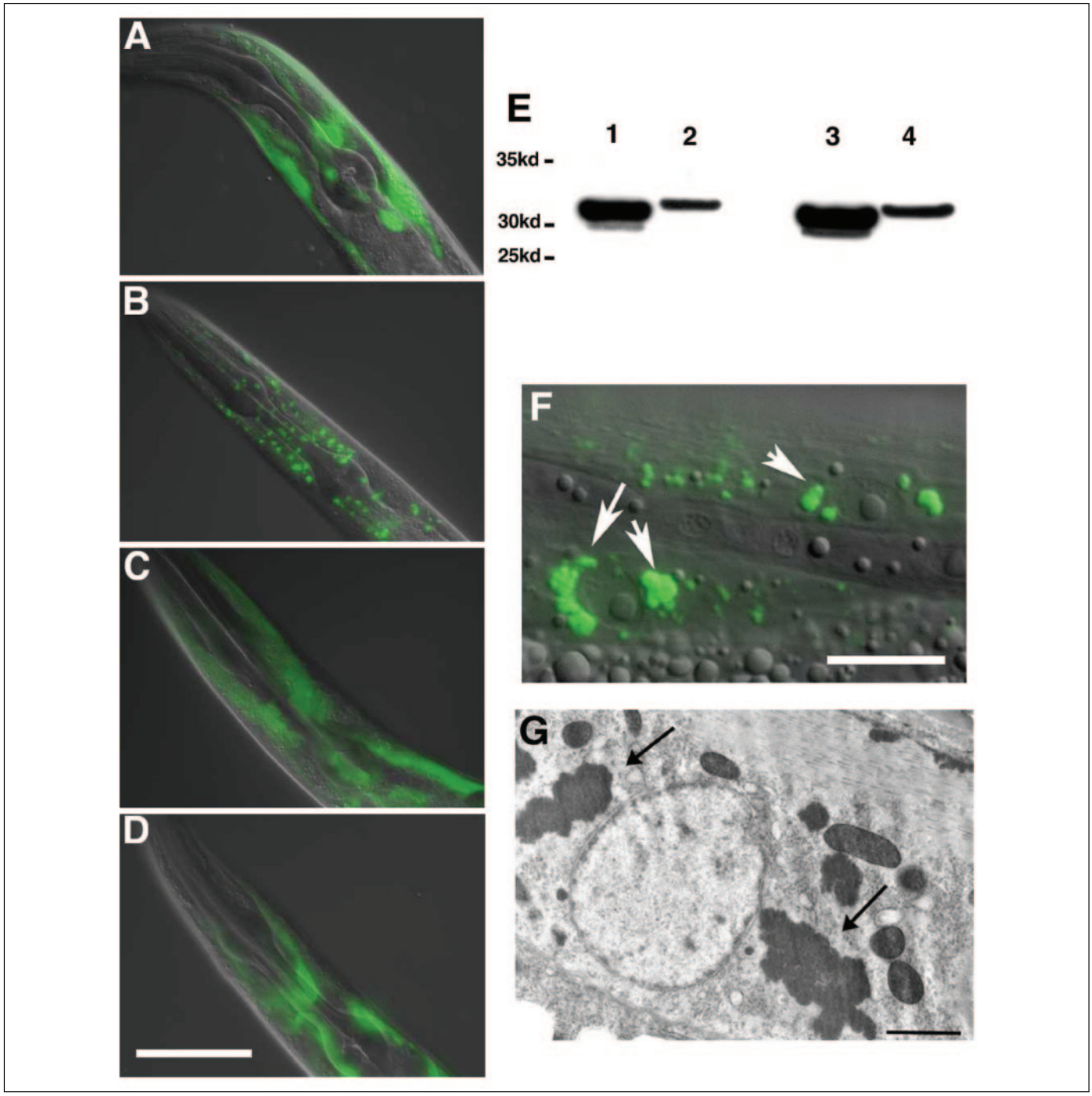

FIGURE 1. **Formation of perinuclear aggregates by GFP::degron in *C. elegans*.** Body wall muscle expression of unmodified GFP (*A*, strain CL2179), GFP::control peptide (*C*, strain CL1291), and GFP::PEST (*D*, strain CL1399) results in diffuse, cytoplasmic fluorescence. Body wall muscle expression of GFP::degron results in the formation of fluorescent aggregates (*B*, strain CL2292). *E*, quantitative anti-GFP immunoblot with lysates from CL2179 (*lanes 1* and *3*) and CL2292 (*lanes 2* and *4*). Gel was loaded with formic acid extracts of 5 μg (*lanes 1* and *2*) or 25 μg (*lanes 3* and *4*) of total protein. See supplemental Fig. 1*A* for corresponding Ponceau S total protein stain of this immunoblot. *F*, high magnification image of perinuclear fluorescent aggregates (*arrows*) in GFP::degron strain CL2292. *G*, electron micrograph of muscle cells expressing GFP::degron. Note perinuclear electron-dense deposits (*arrows*). *A–D*, living animals, digitally fused differential interference contrast (*DIC*) and epifluorescence (projected digitally deconvolved) images, *size bar* = 50 μm. *F*, live animal, digitally fused DIC and epifluorescence images, *size bar* = 10 μm. *G*, *size bar* = 1 μm.

AB5622) antibody overnight at 4 °C (to identify neurons), which was followed by incubation in Cy3-conjugated goat anti-rabbit (1:500, The Jackson Laboratory) for 1 h at 37 °C. Coverslips were mounted on glass slides in Elvanol containing 0.5 mg/ml DAPI. Images of GFP-expressing cells were acquired using a SPOT RT-SE (Diagnostics Instruments) cooled CCD camera controlled by Metamorph software (Universal Imaging) with a −60, 1.4 N.A. Plan Apo objective (Nikon).

Electron Microscopy—Synchronously hatched cultures of transgenic nematodes were propagated at 16 °C for 36 h and then up-shifted as third larval stage animals to 25 °C for 24 h to induce transgene expression, as described previously (15). Aliquots of induced fourth larval stage animals were frozen in a Balzers HPM 010 high pressure freezing apparatus as described previously (16). Samples were freeze-substituted in 2% osmium tetroxide and 0.05% uranyl acetate in acetone at −80 °C for

5 days, gradually warmed to room temperature, infiltrated with Araldite/Embed-812 (Electron Microscopy Sciences), and polymerized. Thin sections were stained with 2% uranyl acetate and Reynold's lead citrate and imaged at 80 kV in a JEOL 100C or Phillips CM10 electron microscope.

Sequential Extraction of Nematode Homogenates—Homogenates were prepared as described previously for immunoprecipitation experiments (17) from equivalent size populations of transgenic worms and then extracted in 100 mM Tris, pH 8.6, 10% glycerol for 1 h at 4 °C in the presence of protease inhibitors. Insoluble material was pelleted (25,000 × *g* for 15 min) and then re-extracted in 1% SDS for 1 h at 4 °C. The remaining insoluble material was pelleted (25,000 × *g* for 15 min) and solubilized in 70% formic acid. Extracts were concentrated and desalted using Microcon centrifugal filter tubes (Millipore), fractionated on a NOVEX 4–12% BisTris gel using MES SDS running buffer (Invitrogen), transferred to nitrocellulose, stained with Ponceau S to confirm that loading and transfer had been equivalent for all of the extracts, and immunoblotted with anti-GFP antibody (Qbiogene) (see supplemental Fig. S1).

Filter Trap Assays—Worm lysates were prepared using a Tris/Triton X-100 immunoprecipitation buffer as described previously (17). Lysates were centrifuged at 2,000 rpm in a microcentrifuge (325 relative centrifugal force) for 5 min to remove large insoluble material (cuticle fragments, etc.), and the supernatant was saved as the lysate supernatant. Gel fractionation of the lysate supernatants and subsequent Ponceau S staining were used to equalize levels of total protein between lysates. 30-μl aliquots of lysate supernatant were run through a cellulose acetate membrane (0.2 μm) pre-soaked in Tris/Triton X-100 immunoprecipitation buffer using vacuum pressure. The membranes were allowed to dry, and then the individual sample dots were placed into separate wells of a 96-well microtiter plate (clear, flat bottom wells). Total GFP fluorescence trapped on the membrane was quantified using a Tecan GENios microplate reader (485 nm excitation and 535 nm emission filters).

Immunoprecipitation Studies—Magnetic μbeads (Miltenyi Biotec) were cross-linked to anti-GFP 3E6 antibody (Qbiogene) and purified using a magnetized column (Miltenyi Biotec). Purified μbeads were mixed with 0.5 ml of worm lysate prepared as described previously (17). After incubation, the lysate/μbead mixture was run through a magnetized column to purify the immunoprecipitate. This protocol involves no centrifugation or sedimentation, thereby avoiding nonspecific recovery of particulate material (*e.g.* protein aggregates). The μMAC immunoprecipitate was washed four times with lysis buffer (1% Triton), once with 50 mM Tris, pH 7.5, and then eluted using a small volume of 95 °C Laemmli Sample Buffer (4% SDS). The μMAC immunoprecipitation eluate was run on a 12% BisTris gel using MES running buffer (Invitrogen) and immunoblotted with anti-GFP and anti-HSP-16 antibodies.

Scoring of Transgenic Worm Paralysis—Populations of transgenic worms were staged by a 2-h synchronous egg lay on 5-cm nematode growth media plates spotted with RW2 strain *Escherichia coli*. Worms were propagated at 16 °C for 48 h after the end of the egg lay and then shifted to 25 °C to induce transgene expression. Scoring for paralysis was initiated 20 h after temperature upshift. Animals were scored as paralyzed if they were associated with "halos" of cleared *E. coli* lawn around their heads (indicative of an insufficient body movement to access food) or if the animals did not move in response to prodding with a tapered platinum wire. Paralyzed animals were removed from the *E. coli* lawn at every time point to facilitate accurate counts of paralyzed animals.

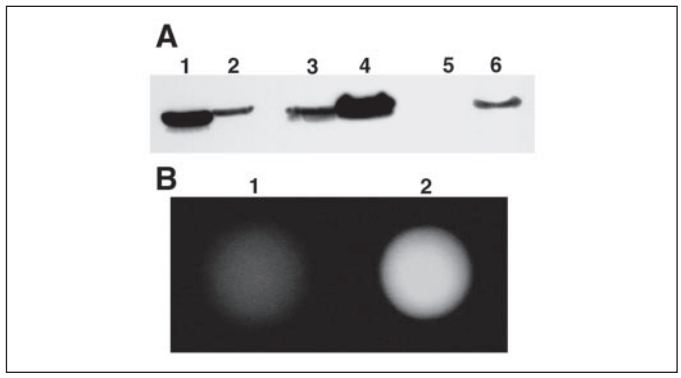

FIGURE 2. **GFP::degron expressed *in vivo* is less soluble than GFP.** *A*, homogenized extracts of CL2179 (GFP, *lanes 1, 3,* and *5*) and CL2292 (GFP::degron, *lanes 2, 4* and *6*) subjected to sequential extraction with Tris/glycerol (*lanes 1* and *2*), 1% SDS buffer (*lanes 3* and *4*), and formic acid (*lanes 5* and *6*) and then fractionated by SDS-PAGE and immunoblotted with anti-GFP antibody. Note the increased fraction of GFP requiring detergent and formic acid solubilization in extracts from GFP::degron-expressing animals (*lanes 4* and *6*). See supplemental Fig. 1*B* for corresponding Ponceau S total protein stain of this immunoblot. *B,* Tris/Triton X-100 lysates from CL2179 (GFP, *spot 1*) and CL2292 (GFP::degron, *spot 2*) run through 0.2-μm cellulose acetate filters. Note the ~8-fold increase in retained fluorescence for GFP::degron-expressing strain.

RESULTS

GFP::Degron Aggregates in C. elegans Muscle—We fused the 16-residue CL1 peptide identified by Gilon *et al.* (11) to the C terminus of GFP and independently expressed either this fusion protein or control GFP in *C. elegans* body wall muscle using the promoter of the *myo-3* gene. Unlike unmodified GFP, which is observed throughout the muscle cytoplasm (Fig. 1*A*), expression of GFP::degron results in perinuclear aggregates, with little detectable diffuse cytoplasmic staining (Fig. 1, *B* and *F*). To determine the specificity of this effect, transgenic lines were generated expressing GFP fused to an out-of-frame degron peptide (Fig. 1*C*) or to the well characterized PEST domain of mouse ornithine decarboxylase (Fig. 1*D*). These control fusions displayed a cytoplasmic distribution like unmodified GFP. To investigate whether the aggregation of GFP::degron might be an artifact of exceptionally high level expression, total (formic acid-extractable) GFP levels were measured by quantitative immunoblot. As shown in Fig. 1*E*, the transgenic strain expressing unmodified GFP (*lanes 1* and *3*) has at least three times as much transgenic protein as does the strain expressing GFP::degron (*lanes 2* and *4*). Thus, the aggregates observed in the GFP::degron strain are because of some qualitative difference between the GFP::degron fusion protein and GFP. To examine these GFP::degron aggregates at the ultrastructural level, the GFP::degron strain was analyzed by high pressure freeze electron microscopy. As shown in Fig. 1*G*, we observed electron-dense, perinuclear deposits specifically in the muscle cells expressing GFP::degron. These cytoplasmic deposits are not membrane-bound and resemble aggresomes (18).

To determine whether the formation of visible GFP::degron aggregates coincided with the production of less-soluble forms of GFP, homogenates of transgenic worms expressing GFP or GFP::degron were subjected to sequential extraction using Tris/glycerol, 1% SDS, and formic acid buffers. As shown in Fig. 2*A*, only a small fraction of GFP::degron is extractable in the Tris/glycerol buffer (compare *lanes 1* and *2*), and only GFP::degron expression results in the formation of a pool of SDS-insoluble, formic acid-extractable material (compare *lanes 5* and *6*). Detergent-resistant GFP::degron aggregates were also observed in filter-trap assays using 0.2-μm pore cellulose acetate filters (Fig. 2*B*). Quantification of retained fluorescence in replicate samples demonstrated that ~8-fold more GFP::degron was retained on the fil-

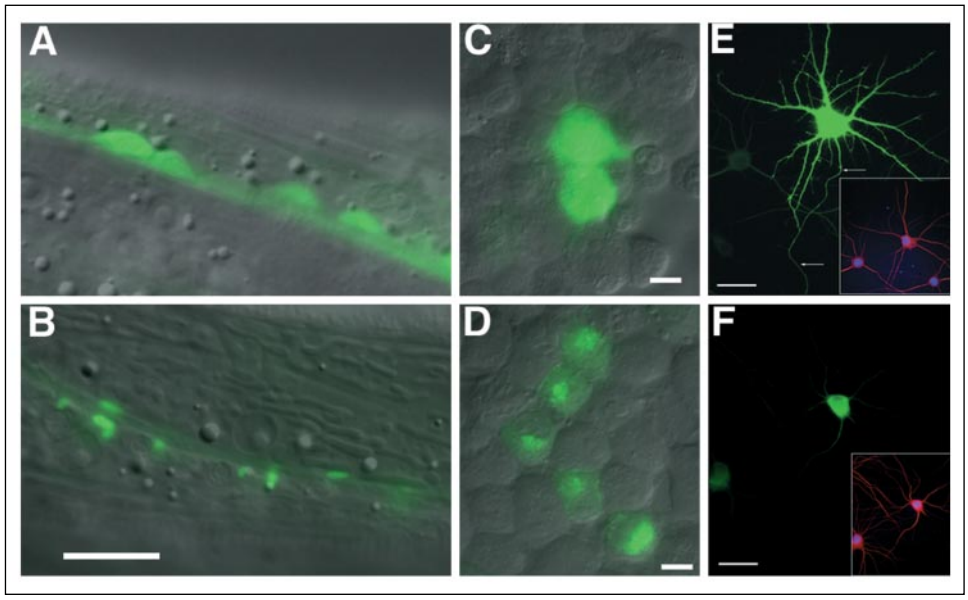

FIGURE 3. **Distribution of GFP::degron in *C. elegans* neurons and mammalian cells in culture.** Living *C. elegans* ventral cord neurons expressing unmodified GFP (*A*) or GFP::degron (*B*). Live mouse N2A cells transfected with control unmodified GFP (pEGFP-C2) (*C*) or GFP::degron construct (pCL85) (*D*). Primary rat hippocampal neurons transfected with EGFP (*E*) or GFP::degron (*F*), fixed, and probed with anti-MAP2 antibody and DAPI (GFP fluorescence shown in *main panel*, MAP2 staining shown in *inset*). Note restricted GFP::degron distribution in all cell types. *A–D,* digitally fused DIC/epifluorescence images. *Size bars,* 10 μm (*A* and *B*) and 25 μm (*C* and *D*).

TABLE 1

End sequences of control and fusion proteins used in this study

Shown are the predicted end amino acid sequences of wild type GFP, expression vector GFP derivatives (pPD118.20 and EGFP-C2), GFP::degron fusions (pAT2, pCL85, and EGFP-u), DsRed(monomer), and DsRed(monomer)::degron fusion. Degron sequences are underlined. Note that unmodified expression vector GFPs contain peptide extensions as a result of the multiple cloning sites introduced into these vectors. These peptide additions (unlike the degron peptide) do not alter GFP fluorescence or solubility.

GFP	. . . HGMDELYK
GFP (pPD118.20)	. . . HGMDELYKSPQALEFASRPYK
GFP::degron (pAT2)	. . . HGMDELYKSPQALEFACKNWFSSLSHFVIHL
GFP::control peptide	. . . HGMDELYKSPQALEFGIRMQELVL
GFP::PEST	. . . HGMDELYKSPQALEFSRPMWQLMKQIQSH GFPPEVEEQDDGTLPMSCAQESGMDRHPAACASARINV
pEGFP-C2	. . . LGMDELYKSGRTQISSSSFEFCSRRYRGPGIHRI
EGFP::degron	. . . LGMDELYKSGRTQISSSSFEFACKNWFSSLSHFVIHL
EGFP-u	. . . LGMDELYKSGLRSRAQASNSAVDGTACKNWFSSLSHFVIHL
DsRed monomer	. . . RHSGSQ
DsRed::degron	. . . RHSGSQVAAATLEFACKNWFSSLSHFVIHL

ters relative to unmodified GFP (16,289 ± 635 S.E. for GFP::degron *versus* 1890 ± 254 S.E. for GFP, relative fluorescence units).

GFP::Degron Aggregation Occurs in Neurons and Mammalian Cells—Given the unexpected aggregation of GFP::degron in *C. elegans* muscle, we first investigated whether this fusion protein would also aggregate in *C. elegans* neurons. As shown in Fig. 3 (*A* and *B*), GFP that is expressed in ventral cord neurons is observed throughout the cell body and axons, whereas GFP::degron forms intense perinuclear deposits in the same neurons. We then asked whether GFP::degron would also aggregate in mammalian cells. The degron peptide was fused to EGFP in a CMV promoter-driven expression vector, and the resulting construct was used to transiently transfect undifferentiated mouse N2A cells and primary fetal rat hippocampal neurons. In both instances, transient GFP::degron expression resulted in perinuclear fluorescence different from the diffuse cytoplasmic fluorescence typically observed in cells transformed with control GFP (compare Fig. 3, *C* and *E* with *D* and *F*).

Transfection of HEK 293 Cells with Degron Fusion Constructs—The results described above differ from the reported fate of GFP::degron fusion protein GFP-u in HEK 293 cells (12). To determine whether this might be because of either cell type differences or subtle differences in the fusion protein sequences (see Table 1 for a comparison of GFP::degron and GFP-u terminal sequences), we transfected HEK 293 cells in parallel with GFP, GFP::degron, and GFP-u. The fraction of transfected cells containing visible aggregates was then scored 17 h after transfection. Cells transfected with either our GFP::degron construct or the previously described GFP-u construct had significantly more transfected cells with visible aggregates than cells transfected with GFP (Fig. 4, *A, C,* and *E*, quantified in *I*). However, GFP itself was seen to occasionally form aggregates in transiently transfected cells (Fig. 4*E*), suggesting that GFP has a native capacity to aggregate when expressed at high levels in HEK 293 cells. This background aggregation of GFP complicates interpretation of the increased rates of GFP::degron and GFP-u aggregation. We therefore fused the degron peptide to DsRed(monomer) (19), which in our hands is much less aggregation-prone than GFP in HEK 293 cells. As shown in Fig. 4 (*G* and *H*, quantified in *I*), addition of the degron peptide to the DsRed(monomer) results in a dramatic increase (~10-fold) in the fraction of transfected cells with aggregates, strongly supporting the view that fusion of proteins to the degron peptide predisposes them to aggregate.

Interaction of GFP::Degron with Chaperone Protein HSP-16—We have shown previously (20) that expression of the aggregation-prone human Aβ peptide in *C. elegans* muscle results in the formation of immunoreactive deposits, often with a perinuclear distribution similar to that of GFP::degron. Aβ expression also results in the induction and co-localization of the small heat shock protein HSP-16, a chaperone protein homologous to αB-crystallin. To determine whether GFP::degron expression has a similar effect on HSP-16 expression and

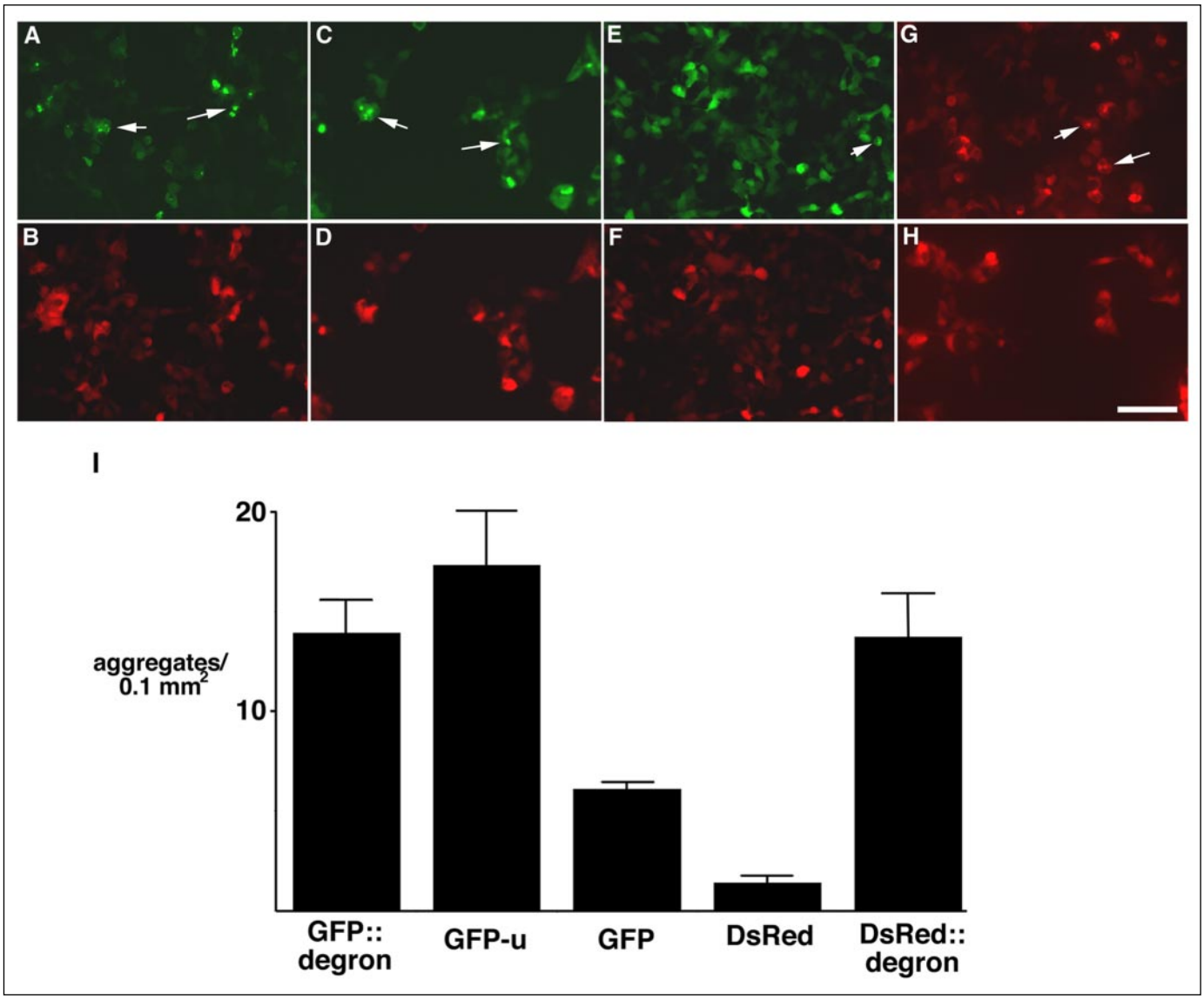

FIGURE 4. **Distribution of degron fusion proteins in HEK 293 cells.** HEK 293 cells were transfected in parallel with plasmids expressing EGFP::degron, EGFP-u, EGFP, DsRed(monomer), or DsRed(monomer)::degron, fixed 17 h after transfection, and then imaged and scored for cells containing aggregates. *A* and *B*, representative field of cells co-transfected with EGFP::degron and DsRed(monomer). Note GFP aggregates (*arrows, A*) in cells with diffuse DsRed fluorescence. *C* and *D*, representative field of cells co-transfected with EGFP-u and DsRed(monomer). Note GFP aggregates (*arrows, C*) in cells with diffuse DsRed fluorescence. *E* and *F*, representative field of cells co-transfected with EGFP and DsRed(monomer). Note more intense overall GFP fluorescence relative to EGFP::degron-transfected cells, and occasional aggregate (*arrow, E*). *G* and *H*, representative fields of cells transfected with DsRed(monomer)::degron (*G*) or DsRed(monomer) (*H*). (Co-transfection with EGFP was not used in this experiment to exclude any influence of occasional EGFP aggregation on DsRed(monomer).) Note aggregates in DsRed(monomer)::degron-transfected cells (*arrows, G*). *I*, quantitation of aggregates. At least three fields (×10 objective) were scored for each of three independent transfection experiments (only two independent experiments for the EGFP-u transfections) using the described criteria (see "Experimental Procedures"). Aggregate values were normalized to total transfected cells area. Note significant increase in aggregate formation for all transfections with degron-containing proteins. *Error bars* = S.E., *size bar* = 100 μm.

localization, a population of CL2292 (*myo-3*/GFP::degron) animals was probed with anti-HSP-16 antibody. As shown in Fig. 5, GFP::degron expression likewise results in the induction of HSP-16 and its transient co-localization with the protein aggregates. The association of HSP-16 with GFP::degron aggregates was seen predominantly in young larval animals with weakly fluorescent GFP aggregates. As evident in the fused image (Fig. 5*B*), although a clear co-localization of GFP fluorescence and HSP-16 immunoreactivity was observed, there was not a one-to-one correspondence between the intensity of the GFP fluorescence and anti-HSP-16 signal, with some weakly fluorescent GFP deposits showing strong HSP-16 immunoreactivity and vice versa. To investigate further the nature of the association of GFP::degron and HSP-16, GFP::degron and control GFP protein were immunoprecipitated from populations of transgenic worms, fractionated, and probed with anti-HSP-16 antibody. HSP-16 was co-immunoprecipitated much more strongly with GFP::degron than with GFP (Fig. 5*D*). (Consistent with this, we have shown previously that endogenous HSP-16 induced by heat shock is not efficiently co-immunoprecipitated with GFP (17).) As the immunoprecipitation experiments were performed under conditions that preserved the GFP::degron aggregates in the worm lysates, these studies demonstrated the association of HSP-16 with the aggregates but did not prove direct binding of HSP-16 to GFP::degron.

Toxicity of GFP::Degron—To assess the cellular toxicity of the GFP::degron *in vivo*, we employed a temperature-inducible expression system previously used for inducible Aβ expression (15). (This approach allows recovery of transgenic animals under low transgene expression conditions, thus preventing selection against lines with high expression of a potentially toxic transgene.) We have demonstrated

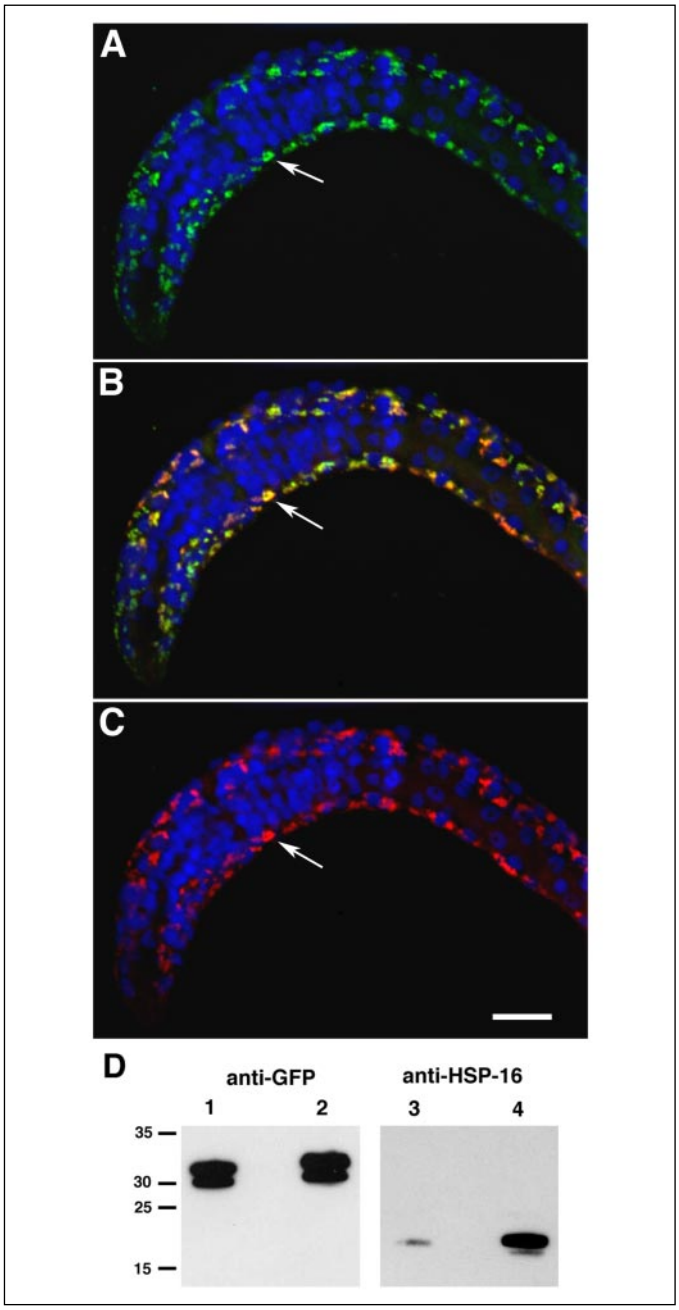

FIGURE 5. **Interaction of GFP::degron with *C. elegans chaperone protein HSP-16.*** Fixed first-stage CL2292 larval animal (*myo-3*/HSP-16.2) imaged for endogenous GFP fluorescence (*A*), HSP-16 immunoreactivity (*C*), and fused fluorescence overlap (*B*). Note co-localization of HSP-16 immunoreactivity and GFP::degron fluorescence (*arrows*). *Size bar* = 10 μm. *D*, immunoblot of anti-GFP immunoprecipitate from CL2179 (unmodified GFP, *lanes 1* and *3*) and CL2292 (GFP::degron, *lanes 2* and *4*) sequentially probed with anti-GFP (*lanes 1* and *2*) and anti-HSP-16 (*lanes 3* and *4*). Note enhanced recovery of HSP-16 immunoreactivity in GFP::degron immunoprecipitates. See supplemental Fig. 1*C* for corresponding Ponceau S total protein stain of this immunoblot.

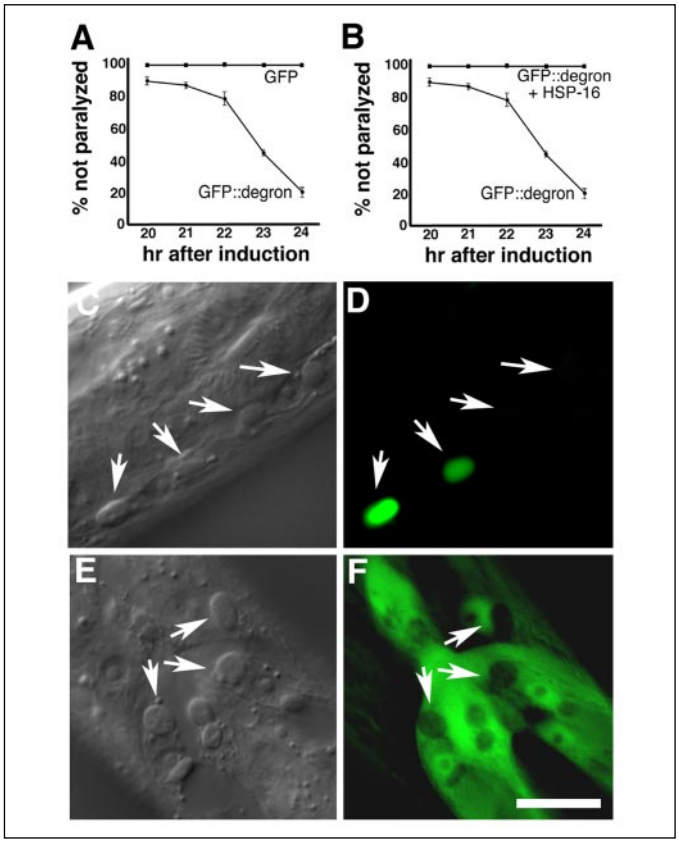

FIGURE 6. **Toxicity of GFP::degron is suppressed by overexpression of HSP-16.** *A*, temperature shift induction of GFP::degron (strain CL2337, $n = 355$) results in significant paralysis after 24 h of induction, which is not observed with induction of GFP (strain CL2179, $n = 448$). *B*, co-expression of HSP-16 suppresses GFP::degron-induced paralysis (dual transgenic strain CL736, $n = 251$). (Data represented in *A* and *B* are from the same experiment but are displayed in two panels to avoid overlap of CL2179 and CL736 plots). *C*, DIC image of living dual transgenic worm with constitutive expression of HSP-16.2 and induced expression of GFP::degron in body wall muscle. Note HSP-16.2 inclusions (*arrows*). *D*, epifluorescence image of dual transgenic worm shown in C. Note sequestration of GFP degron into a subset of HSP-16.2 inclusions. *E*, DIC image of living dual transgenic worm with constitutive expression of HSP-16.2 and induced expression of unmodified GFP in body wall muscle. HSP-16.2 inclusions indicated by *arrows*. *F*, epifluorescence image of dual transgenic worm shown in *E*. Note exclusion of unmodified GFP from HSP-16.2 inclusions (*arrows*). *C–F, size bar* = 10 μm.

previously that temperature induction of Aβ expression in body wall muscle results in robust paralysis ~24 h after upshift. Transgenic lines were engineered in parallel to express unmodified GFP (CL2179) or GFP::degron (CL2337) when induced. Under these conditions, temperature upshift of the inducible GFP::degron strain led to paralysis of ~80% of the population by 24 h, whereas the inducible GFP animals were not paralyzed at this time (Fig. 6*A*). Immunoblot quantitation of total (formic acid-extracted) GFP levels showed that the induced CL2337 strain actually expresses less total GFP than induced CL2179, indicating that the observed paralysis is because of qualitative differences between GFP::degron and GFP (data not shown).

GFP::Degron Subcellular Distribution and Toxicity Are Altered by Overexpression of HSP-16—Co-expression of chaperone proteins can alter the toxicity of aggregation-prone proteins such as Aβ and polyglutamine repeat-containing proteins (21–23). To investigate whether this might also occur with GFP::degron, we generated stable transgenic strains expressing the *hsp-16.2* coding sequence under the control of the *myo-3* muscle-specific promoter, resulting in worms with constitutive expression of HSP-16.2 protein in body wall muscle. This high level constitutive expression of HSP-16.2 results in the formation of muscle-specific HSP-16 inclusions visible by differential interference microscopy (DIC) in living animals.[3] These HSP-16 inclusions have not been observed when endogenous HSP-16 expression is induced (*e.g.* by heat shock). The *myo-3*/HSP-16.2 transgene was introduced by classic genetic mating into the CL2337 (GFP::degron) and CL2179 (unmodified GFP) backgrounds. Introduction of the *myo-3*/HSP-16 transgene into CL2337 strongly suppressed paralysis resulting from GFP::degron induction (Fig. 6*B*). This suppression was associated with a dramatic

[3] V. Fonte and C. D. Link, manuscript in preparation.

redistribution of GFP::degron into the HSP-16.2 inclusions (Fig. 6, *C* and *D*). Conversely, soluble GFP was excluded from the HSP-16.2 inclusions (Fig. 6, *E* and *F*). This result clearly demonstrates a differential interaction of GFP and GFP::degron with the HSP-16.2 chaperone protein, highlighting the apparent non-native character of the GFP::degron protein.

DISCUSSION

GFP::degron protein fusions (also designated GFP-u) have been used by several groups as an unstable GFP variant to monitor proteasome function (12, 24–26) in mammalian cell culture. We have observed strong aggregation of GFP::degron upon *in vivo* expression in *C. elegans* muscle and neurons, as well as localized deposition of GFP::degron and DsRed(monomer)::degron in transiently transfected mammalian cells. These two sets of observations can be reconciled if C-terminal addition of the degron peptide promotes GFP misfolding or multimerization, resulting in a protein that is both aggregation-prone and subject to enhanced chaperone-mediated proteasomal degradation. In this model, the fate of GFP::degron (aggregation *versus* degradation) depends upon the balance of transgene expression and the capacity of a given cell type to degrade non-native proteins.

An alternative model is that the degron peptide acts as a specific proteasome targeting signal (*e.g.* analogous to a PEST domain), and the aggregates we observe occur because proteasomal function is overwhelmed by engagement with GFP::degron. We do not favor this model because of the following: 1) it does not account for the reduced solubility of GFP::degron in our biochemical assays, 2) it does not account for the specific interaction of GFP::degron with the HSP-16 chaperone protein, 3) an equivalent GFP::PEST fusion construct does not form aggregates in *C. elegans* muscle, 4) inhibition of proteasomal function by RNA interference of specific proteasomal subunits does not lead to aggregation of soluble GFP in *C. elegans* muscle (although this treatment does lead to enhanced aggregation of a GFP::Gln-35 polyglutamine repeat reporter protein) (27).

It is surprising that a relatively minimal addition of 16 residues to the C terminus of GFP can convert this normally soluble protein into a strongly aggregating one. This observation is in stark contrast to the many examples where GFP fusion proteins remain soluble or assume the cellular distribution of the partner fusion protein (28). The capacity of the degron peptide to induce GFP aggregation suggests that this peptide may have some unique structural characteristic. Overall, the degron peptide is not strongly hydrophobic, but it is predicted to form an almost perfect amphipathic α-helix. It is conceivable that degron addition leads to protein multimerization, perhaps driven by pairing of the hydrophobic and hydrophilic faces of the amphipathic helix. Alternatively, the C-terminal degron might directly interfere with GFP folding, resulting in misfolded (but still fluorescent) forms predisposed to aggregate.

We have shown that GFP::degron can be toxic when expressed in *C. elegans* muscle cells, as has been demonstrated previously for Aβ (5) and GFP::polyglutamine fusions (6). We have not observed any muscle cell changes by light or electron microscopy associated with GFP::degron expression that suggest a mechanism for this cell toxicity. However, it does not appear that this toxicity involves a classic apoptotic pathway (we see no indications of chromatin fragmentation by electron microscopy) or gross cellular damage. The large range of molecular and genetic tools available in *C. elegans* (*e.g.* suppressor screens) should enable us to identify components of GFP::degron toxicity, which we anticipate will be relevant to protein aggregation toxicity in general. Although the paralysis phenotypes induced by Aβ and GFP::degron are grossly similar, these toxic proteins may still act through different or partially overlapping cellular and molecular mechanisms.

The transient association of HSP-16 with GFP::degron suggests that this chaperone protein may interact only with an initial form of GFP::degron aggregate, perhaps an oligomer. This seemingly aggregation stage-specific interaction of HSP-16 and GFP::degron may be analogous to the observation that HSP-16 does not co-localize with fully fibrillar β-amyloid (17). In *C. elegans* animals induced to express Aβ, oxidative damage and gross toxicity precede amyloid formation (29), consistent with the growing body of evidence that prefibrillar oligomers may be the key toxic species for Aβ and other disease-associated proteins (30). Similarly, the initial form of GFP::degron bound by HSP-16 may be the critical toxic species of GFP::degron, not the strongly fluorescent, mature GFP::degron aggregates. The mechanism(s) by which HSP-16 overexpression suppresses GFP::degron aggregation and toxicity are currently under investigation. Of particular interest is whether the secondary or tertiary structure of GFP::degron associated with HSP-16 inclusions is different from its structure when it is deposited in perinuclear aggregates.

Interpretation of studies employing transgenic expression of specific disease-associated aggregating proteins would be enhanced if these studies included controls for the general effects of aggregating protein expression. There have been previous demonstrations of cellular toxicity resulting from exposure to nondisease-associated aggregating proteins or protein fragments, including the N-terminal domain of the *E. coli* HypF protein (31), the Src homology 3 domain of phosphatidylinositol 3-kinase (32), and endostatin (33). However, these studies involved exposing tissue culture cells to *in vitro* aggregated (fibrillar or pre-fibrillar) protein, not endogenous expression. Garcia-Mata *et al.* (34) have shown that fusion of the first 252 residues of membrane-associated transport factor p115 to the C terminus of GFP (GFP-250) results in an aggregating protein that forms aggresomes when expressed in COS7 cells, but they did not report on the toxicity of this fusion protein. We suggest that the GFP::degron protein is an appropriate aggregation control for transgenic *C. elegans* models, and possibly for transgenic models of aggregating protein diseases in general.

Acknowledgments—We thank A. Fire for providing C. elegans expression vectors and R. Kopito for providing the original GFP-u construct and sequence. We also thank Andrew Taft for the construction of some expression plasmids and Justin Springett for media preparation. Some nematode strains were provided by the Caenorhabditis Genetics Center, funded by the National Institutes of Health National Center for Research Resources.

REFERENCES

1. Stefani, M., and Dobson, C. M. (2003) *J. Mol. Med.* **81,** 678–699
2. Taylor, J. P., Hardy, J., and Fischbeck, K. H. (2002) *Science* **296,** 1991–1995
3. Price, D. L., Wong, P. C., Markowska, A. L., Lee, M. K., Thinakaren, G., Cleveland, D. W., Sisodia, S. S., and Borchelt, D. R. (2000) *Ann. N. Y. Acad. Sci.* **920,** 179–191
4. Link, C. D. (2001) *Mech. Ageing Dev.* **122,** 1639–1649
5. Link, C. D. (1995) *Proc. Natl. Acad. Sci. U. S. A.* **92,** 9368–9372
6. Morley, J. F., Brignull, H. R., Weyers, J. J., and Morimoto, R. I. (2002) *Proc. Natl. Acad. Sci. U. S. A.* **99,** 10417–10422
7. Parker, J. A., Connolly, J. B., Wellington, C., Hayden, M., Dausset, J., and Neri, C. (2001) *Proc. Natl. Acad. Sci. U. S. A.* **98,** 13318–13323
8. Faber, P. W., Alter, J. R., MacDonald, M. E., and Hart, A. C. (1999) *Proc. Natl. Acad. Sci. U. S. A.* **96,** 179–184
9. Lakso, M., Vartiainen, S., Moilanen, A. M., Sirvio, J., Thomas, J. H., Nass, R., Blakely, R. D., and Wong, G. (2003) *J. Neurochem.* **86,** 165–172
10. Kraemer, B. C., Zhang, B., Leverenz, J. B., Thomas, J. H., Trojanowski, J. Q., and Schellenberg, G. D. (2003) *Proc. Natl. Acad. Sci. U. S. A.* **100,** 9980–9985
11. Gilon, T., Chomsky, O., and Kulka, R. G. (1998) *EMBO J.* **17,** 2759–2766
12. Bence, N. F., Sampat, R. M., and Kopito, R. R. (2001) *Science* **292,** 1552–1555
13. Banker, G., and Goslin, K. (eds) (1998) *Culturing Nerve Cells,* 2nd Ed., MIT Press, pp. 339–370, Cambridge, MA

14. Hockertz, M. K., Clark-Lewis, I., and Candido, E. P. (1991) *FEBS Lett.* **280,** 375–378
15. Link, C. D., Taft, A., Kapulkin, V., Duke, K., Kim, S., Fei, Q., Wood, D. E., and Sahagan, B. G. (2003) *Neurobiol. Aging* **24,** 397–413
16. Dahl, R., and Staehelin, L. A. (1989) *J. Electron Microsc. Technol.* **13,** 165–174
17. Fonte, V., Kapulkin, V., Taft, A., Fluet, A., Friedman, D., and Link, C. D. (2002) *Proc. Natl. Acad. Sci. U. S. A.* **99,** 9439–9444
18. Johnston, J. A., Ward, C. L., and Kopito, R. R. (1998) *J. Cell Biol.* **143,** 1883–1898
19. Campbell, R. E., Tour, O., Palmer, A. E., Steinbach, P. A., Baird, G. S., Zacharias, D. A., and Tsien, R. Y. (2002) *Proc. Natl. Acad. Sci. U. S. A.* **99,** 7877–7882
20. Fay, D. S., Fluet, A., Johnson, C. J., and Link, C. D. (1998) *J. Neurochem.* **71,** 1616–1625
21. Auluck, P. K., Meulener, M. C., and Bonini, N. M. (2005) *J. Biol. Chem.* **280,** 2873–2878
22. Magrane, J., Smith, R. C., Walsh, K., and Querfurth, H. W. (2004) *J. Neurosci.* **24,** 1700–1706
23. Bonini, N. M. (2002) *Proc. Natl. Acad. Sci. U. S. A.* **99,** Suppl. 4, 16407–16411
24. Dong, X., Liu, J., Zheng, H., Glasford, J. W., Huang, W., Chen, Q. H., Harden, N. R., Li, F., Gerdes, A. M., and Wang, X. (2004) *Am. J. Physiol.* **287,** H1417–H1425
25. Hope, A. D., de Silva, R., Fischer, D. F., Hol, E. M., van Leeuwen, F. W., and Lees, A. J. (2003) *J. Neurochem.* **86,** 394–404
26. Bennett, E. J., Bence, N. F., Jayakumar, R., and Kopito, R. R. (2005) *Mol. Cell* **17,** 351–365
27. Nollen, E. A., Garcia, S. M., van Haaften, G., Kim, S., Chavez, A., Morimoto, R. I., and Plasterk, R. H. (2004) *Proc. Natl. Acad. Sci. U. S. A.* **101,** 6403–6408
28. Tsien, R. Y., and Miyawaki, A. (1998) *Science* **280,** 1954–1955
29. Drake, J., Link, C. D., and Butterfield, D. A. (2003) *Neurobiol. Aging* **24,** 415–420
30. Walsh, D. M., and Selkoe, D. J. (2004) *Protein Pept. Lett.* **11,** 213–228
31. Bucciantini, M., Calloni, G., Chiti, F., Formigli, L., Nosi, D., Dobson, C. M., and Stefani, M. (2004) *J. Biol. Chem.* **279,** 31374–31382
32. Bucciantini, M., Giannoni, E., Chiti, F., Baroni, F., Formigli, L., Zurdo, J., Taddei, N., Ramponi, G., Dobson, C. M., and Stefani, M. (2002) *Nature* **416,** 507–511
33. Kranenburg, O., Kroon-Batenburg, L. M., Reijerkerk, A., Wu, Y. P., Voest, E. E., and Gebbink, M. F. (2003) *FEBS Lett.* **539,** 149–155
34. Garcia-Mata, R., Bebok, Z., Sorscher, E. J., and Sztul, E. S. (1999) *J. Cell Biol.* **146,** 1239–1254